Available online at www.sciencedirect.com
SCIENCE DIRECT®
Journal of Power Sources 144 (2005) 214–219
JOURNAL OF POWER SOURCES
www.elsevier.com/locate/jpowsour

Short communication

Study of the electrochemical properties of Ga-doped $LiNi_{0.8}Co_{0.2}O_2$ synthesized by a sol–gel method

Chang Joo Han [a], Won Sob Eom [a], Sang Myoung Lee [a], Won Il Cho [b], Ho Jang [a,*]

[a] Department of Advanced Materials Engineering, College of Engineering, Korea University, 5-1 Anam-dong, Seongbuk-gu, Seoul 136-713, South Korea
[b] Eco-Nano Research Center, Korea Institute of Science and Technology, 39-1 Hawolgok-dong, Seongbuk-gu, Seoul 136-791, South Korea

Received 18 October 2004; received in revised form 19 December 2004; accepted 19 December 2004
Available online 21 February 2005

Abstract

The effects of gallium doping on the structure and electrochemical properties of $LiNi_{0.8}Co_{0.2}O_2$ were investigated by X-ray diffraction, cyclic voltammetry and charge-discharge tests. $LiNi_{0.8}Co_{0.2-x}Ga_xO_2$ ($x = 0.01, 0.03, 0.05$) was synthesized using a sol–gel method and it showed the average particle size less than 1 μm in diameter. Results showed that gallium-doping had no effect on the crystal structure (α-$NaFeO_2$) of the cathode material in the range $x \leq 0.05$. On the other hand, two transitions at 3.7–3.9 and 4.2–4.7 V observed during the cycle test were merged into one when the amount of gallium doping increases to 0.05, implying that the enhanced capacity retention with gallium doping is attributed to the suppression of the phase transition of the cathode. However, the increase of gallium content in $LiNi_{0.8}Co_{0.2}O_2$ slightly decreases the initial discharge capacity.

Keywords: Cathode; Sol–gel method; $LiNi_{0.8}Co_{0.2-x}Ga_xO_2$; Phase transition

1. Introduction

Performance of a Li-secondary battery is strongly affected by structural stability of a cathode material, since the amount of lithiation and delithiation of Li ions during the charge and discharge is determined by the atomic configuration of the cathode [1–3]. Numerous candidates such as $LiCoO_2$ [4], $LiNiO_2$ [5], $LiMn_2O_4$ [6,7] and their derivatives have been studied for cathodes with better structural stability and exploration for improved cathode materials has been extended to other oxides [8].

Among many candidates, mostly $LiCoO_2$ has been used as a cathode material for commercial lithium ion batteries since its synthesis is easy and straightforward. However, $LiCoO_2$ has disadvantages in terms of cost, toxicity and electrochemical capacity. On the other hand, $LiNiO_2$ costs less than $LiCoO_2$ and has higher electrochemical capacity while it has a similar layered structure as $LiCoO_2$. However, the cycling behavior of $LiNiO_2$ is poor at high voltages and exhibits thermal instability in its charged states, due to decomposition at elevated temperature. Recently, $LiMn_2O_4$ has attracted attention due to its low cost, high voltage, high thermal stability and non-toxicity. The $LiMn_2O_4$, however, shows capacity fading due to Jahn–teller distortion, dissolution of Mn^{3+} from spinel structure and oxidation of Mn^{4+} in the electrolyte at the high voltage.

Concerning the advantages and disadvantages of $LiCoO_2$ and $LiNiO_2$, $LiNi_{1-x}CoO_2$ ($0 \leq x \leq 1$) compounds have been developed, based on the fact that $LiCoO_2$ and $LiNiO_2$ have the same layered α-$NaFeO_2$-type structure [8–11]. Among them, $LiNi_{0.8}Co_{0.2}O_2$ has shown good electrochemical properties and further improvement in electrochemical properties has been reported by doping elements such as Al, Mn, Fe, Ga and Nb, which partially substitute Ni or Co with the doping elements [12–17]. In particular, gallium has been known as a good candidate material as a dopant since it improves structural stability of $LiNiO_2$ [17]. The gallium doped $LiNiO_2$ has

* Corresponding author. Tel.: +82 2 3290 3276; fax: +82 2 928 3584.
E-mail address: hojang@korea.ac.kr (H. Jang).

0378-7753/$ – see front matter © 2005 Elsevier B.V. All rights reserved.
doi:10.1016/j.jpowsour.2004.12.021

a single hexagonal phase and its lattice parameters change slowly and continuously during charge–discharge processes. The hexagonal structure is maintained and no other structure has been observed during the charge–discharge processes. The studies of the electrochemical properties of Ga-doped Li-secondary batteries with different compositions are also available in the literature. Co-doping of Ga and Mg on the $LiNiO_2$ also shows capacity improvement due to suppression of the phase transition [18]. Kim et al. [19] synthesized the $LiNi_{1-x-y}Co_xGa_yO_2$ by solid-state reaction and achieve the discharge capacity above 190 mAh g^{-1} at 3.0–4.2 V range. They attribute the high discharge capacity of the $LiNi_{1-x-y}Co_xGa_yO_2$ to the substitution of Ni^{3+} with Ga^{3+}. In situ X-ray absorption spectroscopy (XAS) study of local structure of Ga ions in $LiNi_{0.908}Co_{0.085}Ga_{0.003}O_2$ cathode suggests that the high stability of Ga in tetrahedral sites is the reason for the significant improvement of the electrochemical properties [20]. Similar results showing structural stability of gallium doped $LiCoO_2$ and $LiMn_2O_4$ are also reported, suggesting possible improvement of electrochemical properties of Li-batteries [21–23].

In this study, the structure and electrochemical properties of the $LiNi_{0.8}Co_{0.2-x}Ga_xO_2$ (x = 0.00, 0.01, 0.03, 0.05) were investigated by substituting Co with Ga. The emphasis of the current investigation was given to the improvement of capacity retention and cycle stability at higher voltage ranges by achieving the homogeneous distribution of gallium in the cathode by employing a sol–gel method.

2. Experimental

The polycrystalline powder with compositions $LiNi_{0.8}Co_{0.2-x}Ga_xO_2$, where x = 0.00, 0.01, 0.03 and 0.05, were produced by a sol–gel method. The gel was formed at 140 °C by mixing $Li(CH_3COO)·2H_2O$, $(CH_3CO_2)_2Ni·4H_2O$ $(CH_3CO_2)_2Co·4H_2O$ and $Ga(NO)_3·xH_2O$ with acrylic acid in the distilled water and fired 800 °C for 24 h in flowing oxygen. The synthesis procedure of $LiNi_{0.8}Co_{0.2-x}Ga_xO_2$ is shown as a schematic diagram in Fig. 1. Composite electrodes were prepared by mixing 84 wt.% of the fine $LiNi_{0.8}Co_{0.2-x}Ga_xO_2$ particles, 10 wt.% KS6 (conductor), and 6 wt.% (polyvinylidene difluoride (PVdF), binder). The mixture was coated on an Al foil, and dried at 80 °C for 24 h.

The charge and discharge characteristics of the cathodes were examined using a laboratory pouch cell. The cell consisted of a cathode, a lithium metal anode and a separator. In this work, 50 cycle tests were performed to examine electrochemical properties of a cathode in a half cell, which is comparable to the charge–discharge tests of more than 200 cycles using the carbon anode in a full cell test. The electrolyte solution was 1 M $LiPF_6$/ethylene carbonate (EC) + ethylmethyl carbonate (EMC) + dimethyl carbonate (DMC). The EC, EMC and DMC were mixed in the volume ratio of 1:1:1. Cells were cycled in the range of 3.0–4.3 and 3.0–4.5 V, and the charge and discharge were carried out at 1/5*C* rate (0.4 mA/cm^2)—first three cycles, 1/3*C* rate-next five cycles and 1/2*C* rate for following cycles.

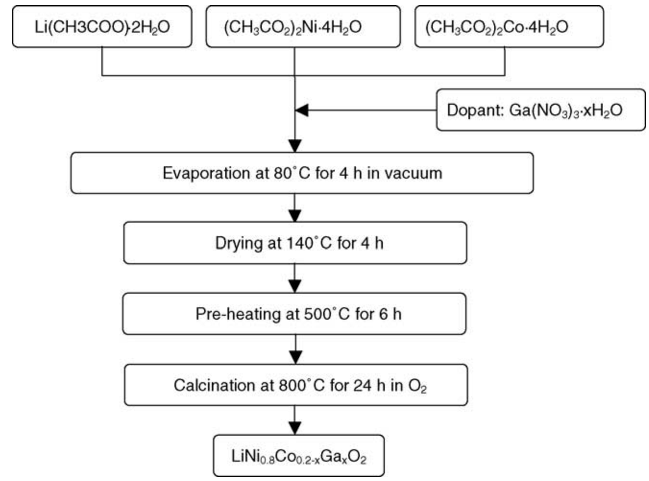

Fig. 1. Experimental procedure for synthesis of $LiNi_{0.8}Co_{0.2-x}Ga_xO_2$ (x = 0.00, 0.01, 0.03 and 0.05) powders by a sol–gel method.

The structure and the morphology of $LiNi_{0.8}Co_{0.2-x}Ga_xO_2$ powders were characterized using various analytical techniques such as X-ray diffraction and scanning electron microscopy. X-ray diffraction experiments were performed with a RINT/DMAX-2500 (RIGAKU/Japan) diffractometer using Cu Kα radiation. The morphological characteristics were observed using a scanning electron microscope (Hitach S-4300).

3. Results and discussion

3.1. Morphology of $LiNi_{0.8}Co_{0.2-x}Ga_xO_2$ powders

The shape and size distribution of the $LiNi_{0.8}Co_{0.2-x}Ga_xO_2$ particles were examined by SEM. $LiNi_{0.2}Co_{0.2}O_2$ powders synthesized by the sol–gel method without doping were consisted of rounded particles with an average size less than 1 μm in diameter (Fig. 2). The average particle size after the same calcination was smaller than the particles synthesized by solid-state reaction methods, implying possible increase of capacity. The small particle size from the sol–gel method was ascribed to the fine initial particles obtained from the sol–gel process. It is reported that the cathodes with fine particles tended to have high initial capacity and low cycle stability and the increase in capacity is attributed to the increase of the surface area, which determines the effectiveness of the lithiation and delithiation processes during charge and discharge of the Li-batteries. On the other hand, better cycle stability with low capacity has been observed in the case of using large particles, due to smaller surface area in the cathode [24].

The SEM micrographs of the $LiNi_{0.8}Co_{0.2-x}Ga_xO_2$ (x = 0.01, 0.03, 0.05) particles are also shown in Fig. 2. The figures indicate that the powders with different Ga contents

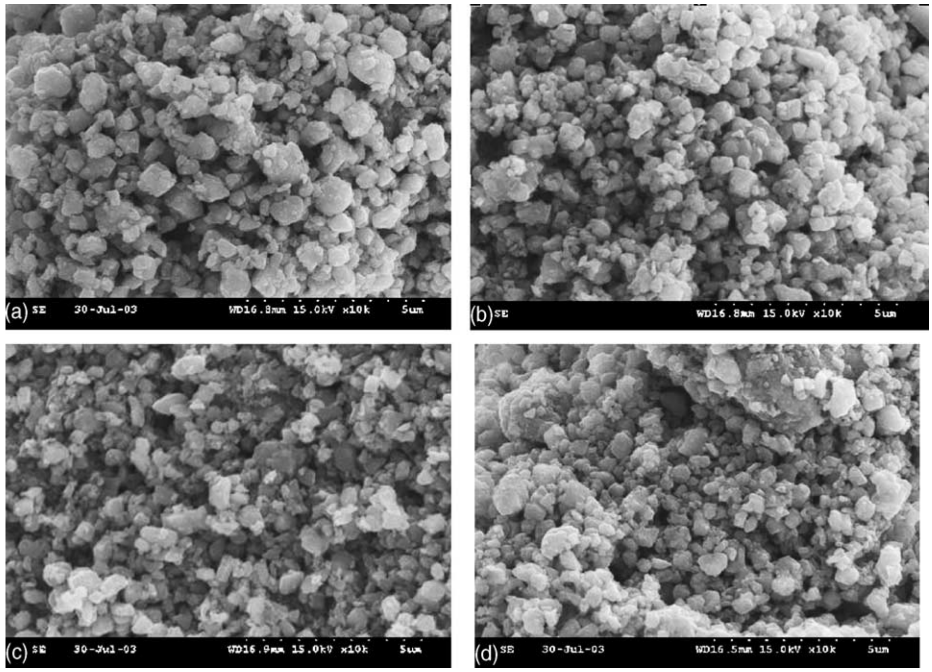

Fig. 2. SEM micrographs of $LiNi_{0.8}Co_{0.2-x}Ga_xO_2$ powders for $x = 0.00$ (a), $x = 0.01$ (b), $x = 0.03$ (c) and $x = 0.05$ (d) synthesized at 800 °C for 24 h in O_2 atmosphere followed by a sol–gel processing.

have the similar size distribution and morphology as the bare $LiNi_{0.8}Co_{0.2}O_2$. This suggests that the gallium is well permeated into the bare $LiNi_{0.8}Co_{0.2}O_2$ forming a solid solution during sol–gel processing. The formation of the solid solution indicates that the gallium ions are homogeneously dissolved into the colloidal precursors in the solution prior to following heat treatments for calcination.

3.2. Structure of the $LiNi_{0.8}Co_{0.2-x}Ga_xO_2$

The structure of the $LiNi_{0.8}Co_{0.2-x}Ga_xO_2$ ($x = 0$, 0.01, 0.03, 0.05) particles was examined by analyzing the X-ray diffraction patterns of the powders that are prepared by sol–gel method. The diffraction patterns (Fig. 3) showed that the structure of the $LiNi_{0.8}Co_{0.2-x}Ga_xO_2$ maintained a layered α-$NaFeO_2$-type structure (space group R-3m). The figure also exhibits a pair of double peaks, (0 0 6)–(1 0 2) and (1 0 8)–(1 1 0) doublets, indicating that Li and Ni/Co are well ordered in a layered structure and the substituted gallium atoms are located in the Ni/Co cation sub-lattices. This result again corroborates the fact that $LiNi_{0.8}Co_{0.2}O_2$ forms a solid solution with gallium atoms, when the $LiNi_{0.8}Co_{0.2-x}Ga_xO_2$ is produced by the sol–gel method.

Fig. 4 shows the ratio (c/a) of the lattice parameters a and c as a function of the gallium content (x) in the $LiNi_{0.8}Co_{0.2-x}Ga_xO_2$. The increase of the ratio (c/a) with gallium addition in this figure is mainly attributed to the increase of c-axis in the hexagonal setting since the lattice parameter along a-axis is negligible compared to the change along c-axis. The increase of the c/a ratio, therefore, indicates the volume expansion of the unit cell and it assists the intercalation and deintercalation of Li ions during electrochemical processes. This result also implies that the gallium atoms are substituted with Ni and Co atoms, and Li cation is restricted around gallium due to the larger ionic radius of gallium than Ni and Co (Ni^{3+} low spin: 0.56 Å, Co^{3+} low spin: 0.54 Å, Ga^{3+}: 0.62 Å) [17,18], resulting in the improvement of the electrochemical properties and structural stability of the cathode. A similar result has been reported in the case of Al addition in $LiNi_{0.8}Co_{0.2}O_2$ [25]. However, different from Al addition, Fig. 4 shows that the volume expansion is saturated with the gallium content, implying that the improvement with the gallium addition for better electrochemical properties of the $LiNi_{0.8}Co_{0.2}O_2$ may have a certain limitation.

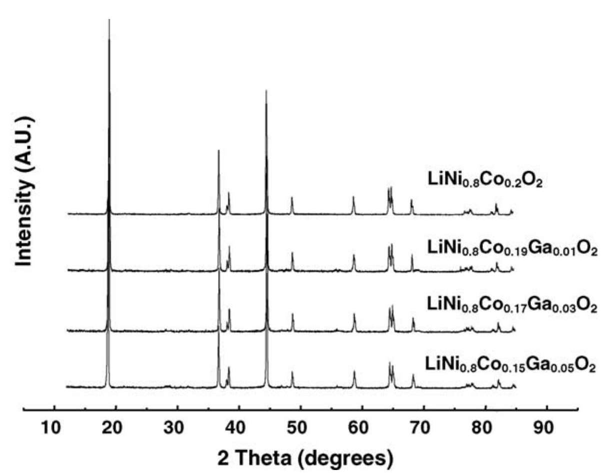

Fig. 3. XRD patterns of $LiNi_{0.8}Co_{0.2-x}Ga_xO_2$ powders for $x = 0.00$, 0.01, 0.03 and 0.05 synthesized by a sol–gel method.

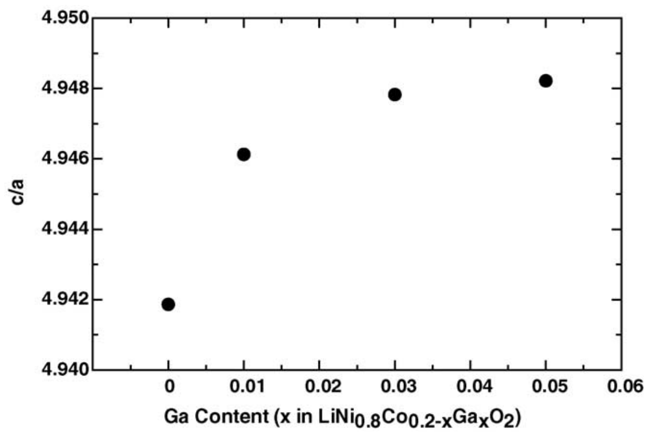

Fig. 4. The change of the lattice parameter ratio (c/a) as a function of the gallium content x in $LiNi_{0.8}Co_{0.2-x}Ga_xO_2$. The lattice parameters c and a are based on the hexagonal setting of a crystal.

3.3. Electrochemical properties of the $LiNi_{0.8}Co_{0.2-x}Ga_xO_2$ particles

Charge–discharge characteristics of the bare $LiNi_{0.8}Co_{0.2}O_2$ and the gallium doped $LiNi_{0.8}Co_{0.2-x}Ga_xO_2$ were investigated by performing cycle tests in the ranges of 3.0–4.3 and 3.0–4.5 V. Fig. 5(a) shows the discharge capacity as a function of the cycle number at 4.3 cut-off voltage. The figure indicates that the initial discharge capacity of the bare $LiNi_{0.8}Co_{0.2}O_2$ is 181.94 mAH g^{-1}, which is higher than the gallium doped $LiNi_{0.8}Co_{0.2-x}Ga_xO_2$. The figure also shows that the initial capacity tends to decrease with gallium doping. However, the bare $LiNi_{0.8}Co_{0.2}O_2$ loses its discharge capacity earlier than the others and shows 49% loss in discharge capacity after 50 cycles. On the other hand, the capacity loss was restrained in the gallium doped $LiNi_{0.8}Co_{0.2}O_2$ and approximately 89% of the initial discharge capacity was maintained after 50 cycles in the case of $LiNi_{0.8}Co_{0.15}Ga_{0.05}O_2$. Similar results were obtained from Ga doped $LiNi_{0.8}Co_{0.18}Ga_{0.02}$ cathodes at the lower voltage range of 3.0–4.2 V [19]. While identical composition of the cathode was seldom found in the literature, the improvement of the capacity retention of the $LiNi_{0.8}Co_{0.2}O_2$ cathode by Ga doping was better than other cathodes with different compositions (Ga addidtion in $LiCoO_2$ [21], $LiMn_2O_4$ [23,26]) and with different doped atoms [31–34].

Fig. 5(b) shows clearer evidence of the gallium role in improving the durability of $LiNi_{0.8}Co_{0.2}O_2$ cathodes. The figure shows the change of the discharge capacity, when the cells were cycled at 3.0–4.5 V. Improved capacity was observed in this case, since the higher cut-off voltage required greater deintercalation of the Li-ions from the layered structure, implying that the structure of the cathode could be rapidly destroyed during cycle tests. The initial capacity of the bare $LiNi_{0.8}Co_{0.2}O_2$ was 223.69 mAH g^{-1} in this case with capacity loss of 69% in 50 cycles. On the other hand, gallium doped $LiNi_{0.8}Co_{0.2-x}Ga_xO_2$ faded slowly and only 12% capacity loss was observed after 50 cycles, suggesting that the gallium improved capacity fading by maintaining the original layered crystal structure during intercalation and deintercalation of Li ions [17–19]. To maintain the structure, a uniform distribution and restriction in the rearrangement of Li ions at a charged state are required. This is because gallium is not a transition metal and rearrangement of Li ions will be restricted by restraining Li ions around the gallium at this state [19]. In this study, a uniform distribution of gallium is obtained by the sol–gel method. Therefore, improved capacity retention is observed at a high cut-off voltage (4.5 V). Fig. 5(a and b) also indicate that the effect of the gallium doping on the stability improvement of $LiNi_{0.8}Co_{0.2}O_2$ is decreased with the gallium amount and not much improvement of cycle characteristics are observed, when x in $LiNi_{0.8}Co_{0.2-x}Ga_xO_2$ is increased from 0.03 to 0.05. This is consistent with the volume expansion of the $LiNi_{0.8}Co_{0.2}O_2$ crystal as a function of gallium content in Fig. 4, since the effect of the gallium dop-

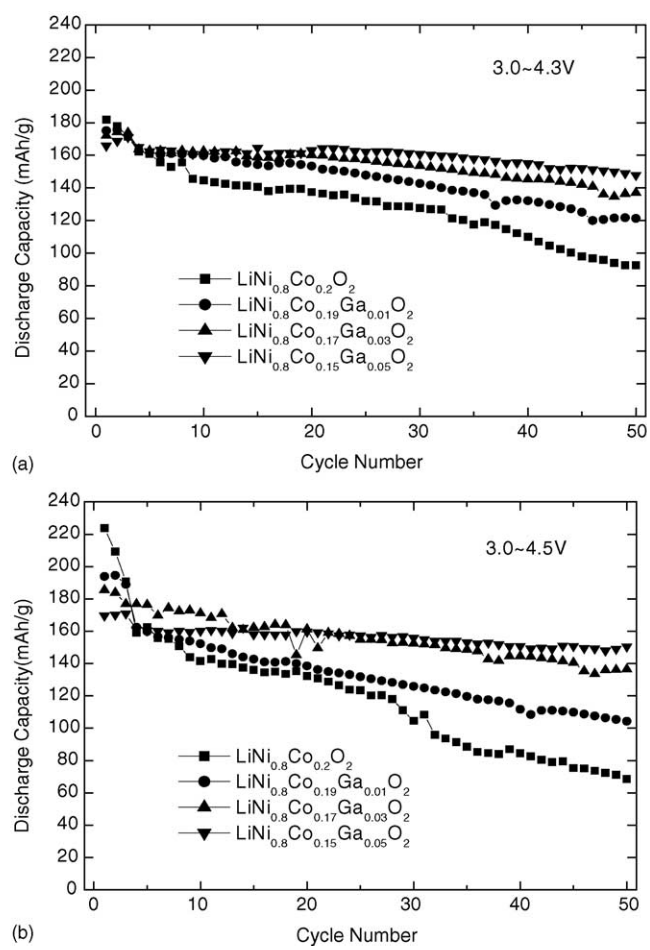

Fig. 5. Plots of discharge capacities of $LiNi_{0.8}Co_{0.2-x}Ga_xO_2$ for $x = 0.00$, 0.01, 0.03 and 0.05 as a function of cycle numbers at two different charge cut-off voltages. The cycle tests were carried out initially by charging and discharging at the 1/5C rate for three cycles, five cycles at the 1/3C rate, and finally at the 1/2C rate for subsequent 42 cycles. Charge and discharge cut-off voltages were between 3.0–4.3 and 3.0–4.5 V at constant charge–discharge current density at room temperature.

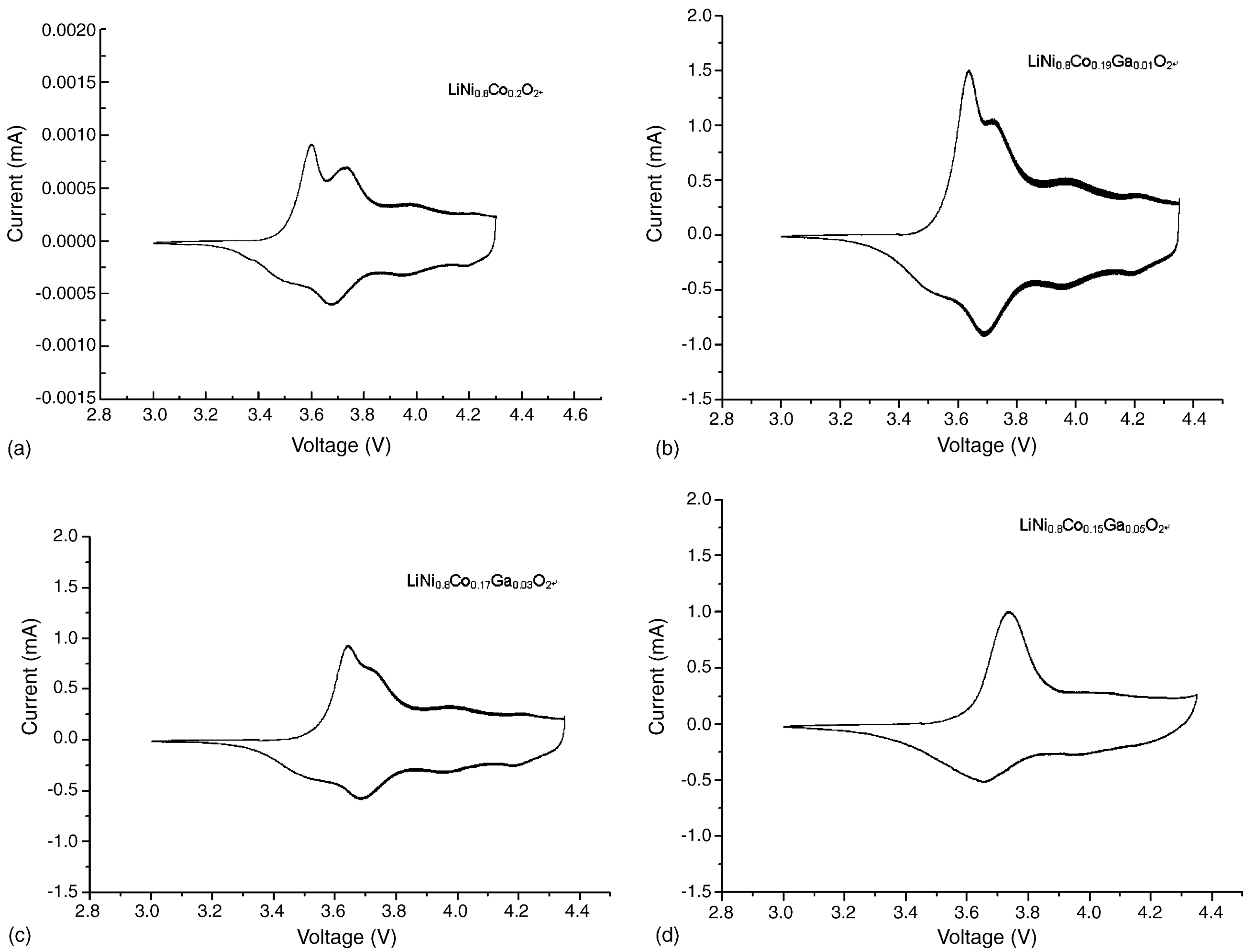

Fig. 6. Cyclic voltammograms obtained from the $LiNi_{0.8}Co_{0.2-x}Ga_xO_2$ powders for $x = 0.00$(a), $x = 0.01$(b), $x = 0.03$(c) and $x = 0.05$(d). Tests were conducted with a pouch-type half-cell containing a Li metal anode and a $LiNi_{0.8}Co_{0.2-x}Ga_xO_2$ cathode. Voltage scan rate was $0.01\ mV\ s^{-1}$.

ing in the lattice parameter along *c*-axis has been reduced as the gallium content is increased.

3.4. Cyclic voltammogram study of the $LiNi_{0.8}Co_{0.2-x}Ga_xO_2$

Cyclic voltammogram (CV) characteristics of the bare $LiNi_{0.8}Co_{0.2}O_2$ and gallium doped $LiNi_{0.8}Co_{0.2-x}Ga_xO_2$ are shown in Fig. 6. This is because the electrochemical properties of the cathode material can be obtained from the presence of the peaks in the CV curve, which provide information about phase transitions during charge–discharge tests [27]. In general, when a cathode experiences phase transformation, a peak appears in the CV curve due to the coexistence of two phases. In the case of $LiCoO_2$, it shows three peaks in the CV curve indicating the existence of four different phases. The first peak appears at 3.9 V, due to the transition from a hexagonal phase (H_1) to another hexagonal phase (H_2). Two other peaks are observed in the CV curve at 4.0 and 4.2 V, which are corresponding to the phase transitions also between hexagonal phase (H_2) and monoclinic phase (M) and between monoclinic phase (M) and hexagonal phase (H_3), respectively [28,29]. $LiNiO_2$ also shows three peaks in the CV curve due multiple phase transitions during CV tests. In this case, peaks due to phase transitions appear at 3.7, 4.0 and 4.2 V, representing the phase transitions of hexagonal phase (H_1) to monoclinic phase (M) at the first peak, monoclinic phase (M) to hexagonal phase (H_2) at the second peak, and hexagonal phase (H_2) to hexagonal phase (H_3) at the third peak [30].

Fig. 6 shows cyclic voltammograms obtained from the bare $LiNi_{0.8}Co_{0.2}O_2$ and gallium doped $LiNi_{0.8}Co_{0.2-x}Ga_xO_2$ ($x = 0.01$, 0.03, 0.05). The CV curve from the bare $LiNi_{0.8}Co_{0.2}O_2$ exhibits three peaks during oxidation indicating the presence of four different phases. The peaks, however, merged into a single peak, when gallium content reaches to $LiNi_{0.8}Co_{0.15}Ga_{0.05}O_2$. The first peak, which eventually merges with a diminishing second peak, shifts from 3.6 to 3.73 V with gallium addition. The simplified CV curve and the peak shift, due to suppression of phase transitions, seem to be well connected with the improved structural stability of the cathode and better capacity retention during cycle tests. Similar results have been reported in the case of gallium doping in the $LiNiO_2$ [17]. They reported that the gallium doping stabilized the crystal structure of the

$LiNiO_2$ during charging process by retaining the hexagonal structures without exhibiting the monoclinic phase which was observed in undoped $LiNiO_2$. On the other hand, our study showed that the structural stability was improved effectively by restricting both the transitions of monoclinic phase and irreversible transitions of hexagonal phase at the high voltage range. Other reports [25,31] also suggest that the improvement of structural stability of $LiNi_{1-x-y}Co_yM_xO_2$ (M = Al, Fe) is attributed to the suppression of phase transitions.

4. Conclusions

Electrochemical properties of the cathode material, $LiNi_{0.8}Co_{0.2-x}Ga_xO_2$ ($x = 0$, 0.01, 0.03 and 0.05), which was synthesized by a sol–gel method, were investigated. The cathode material consisted of fine particles showing an average size less than 1 μm in diameter and it maintained an α-$NaFeO_2$ type (R-3m) layered structure regardless of the gallium content. The lattice parameter along the *c*-axis in the hexagonal setting was increased, while little change was observed in the lattice parameter along *x*-axis, indicating volume expansion due to the increase in inter-slab spacing of the layered structure with gallium doping. However, the expansion along the *c*-axis was lessened when the gallium content reached to $LiNi_{0.8}Co_{0.15}Ga_{0.05}O_2$. The gallium doping improved the capacity retention of $LiNi_{0.8}Co_{0.2}O_2$, while it lowered the initial discharge capacity. The improvement of capacity retention was prominent, when the cycle tests were carried out higher voltage ranges (3.0–4.5 V). Cyclic voltammogram test results suggested that the suppression of the phase transition due to gallium doping induced slow degradation of the discharge capacity of $LiNi_{0.8}Co_{0.15}Ga_{0.05}O_2$ during cycle tests.

Acknowledgement

The research was performed with financial support from the Center for Nanostructure Materials Technology under ‘21st century Frontier R&D Programs’ of the Ministry of Science and Technology, Korea.

References

[1] J.R. Dahn, U. von Sacken, M.W. Juzkow, H. Al-Jannaby, J. Electrochem. Soc. 138 (1991) 2207.
[2] C. Delmas, I. Saadoune, Solid State Ionics 53–56 (1992) 370.
[3] H. Wang, Y. Jang, B. Huang, D. Sadoway, Y. Chiang, J. Electrochem. Soc. 146 (1999) 473.
[4] T. Naganura, K. Tazawa, Prog. Batteries Solar Cells 9 (1990) 20.
[5] W. Ebner, D. Fouchard, L. Xie, Solid State Ionics 69 (1994) 238.
[6] J.M. Tarascon, E. Wang, F.K. Shokoohi, W.R. Mekinnon, S. Colson, J. Electrochem. Soc. 38 (1991) 2859.
[7] T. Ohzuku, M. Kitagawa, T. Hirai, J. Electrochem. Soc. 137 (1990) 769.
[8] J.M. Tarascon, M. Armand, Nature 414 (2001) 359.
[9] J. Saadoune, C. Delmas, Solid State Chem. 136 (1998) 8.
[10] A.G. Ritchie, C.O. Gowa, J.C. Lee, P. Bowles, A. Gilmour, J. Allen, D.A. Rice, F. Brady, S.C.E. Tsang, J. Power Sources 80 (1999) 98.
[11] D. Caurant, N. Baffier, B. Carcia, J.P. Pereira-Ramos, Solid State Ionics 91 (1996) 45.
[12] T. Ohzuku, A. Ueda, M. Kouguchi, J. Electrochem. Soc. 142 (1995) 4033.
[13] A. Rougier, I. Saadoune, P. Gravereau, P. Willmann, C. Delmas, Solid State Ionics 90 (1996) 83.
[14] H. Arai, S. Okada, Y. Sakurai, J. Yamaki, J. Electrochem. Soc. 144 (1997) 3117.
[15] T. Ohzuku, Y. Makimura, Chem. Lett. (2001) 744.
[16] G. Prado, A. Rougier, L. Fournes, C. Delmas, J. Electrochem. Soc. 147 (2000) 2880.
[17] Y. Nishida, K. Nakane, T. Satoh, J. Power Sources 68 (1997) 561.
[18] A. Yu, G.V. Subba, B.V.R. chowdari, Solid State Ionics 135 (2000) 131–135.
[19] W.S. Kim, K.I. Chung, Y.K. Choi, Y.E. Sung, J. Power Sources 115 (2003) 101.
[20] M. Balasubramanian, J. McBreen, K. Pandya, K. Amine, J. Electrochem. Soc. 149 (2002) A1246–A1249.
[21] R. Stoyanova, E. Zhecheva, G. Bromiley, T. Ballaran, R. Alcantara, J. Corredor, J. Tirado, J. Mater. Chem. 12 (2002) 2501–2506.
[22] J.J. Kim, K.H. Ryu, K. Sakaue, H. Terauchi, C.H. Yo, J. Phys. Chem. Solids 63 (2002) 2037.
[23] C. Bellitto, M.G. DiMarco, W.R. Branford, M.A. Green, D.A. Neumann, Solid State Ionics 140 (2001) 77.
[24] J. Cho, B. Park, J. Power Sources 92 (2001) 35.
[25] C.J. Han, J.H. Yoon, W.I. Cho, H. Jang, J. Power Sources 136 (2004) 132.
[26] J.T. Son, H.G. Kim, Y.J. Park, Electrochim. Acta 50 (2004) 453–459.
[27] K. Dokko, M. Nishizawa, S. Horikoshi, T. Itoh, M. Moharmed, I. Uchida, Electrochem. Solid State Lett. 3 (1999) 3.
[28] J.N. Reimers, J.R. Dahn, J. Electrochem. Soc. 139 (1992) 2091.
[29] T. Ohzuku, A. Ueda, J. Electrochem. Soc. 141 (1994) 2972–2977.
[30] W. Li, J.N. Reimers, J.R. Dahn, Solid State Ionics 67 (1993) 123.
[31] K.K. Lee, W.S. Yoon, K.B. Kim, K.Y. Lee, S.T. Hong, J. Power Sources 97–98 (2001) 308–312.
[32] S. Madhavi, G.V. Subba Rao, B.V.R. Chowdari, S.F.Y. Li, J. Power Sources 93 (2001) 156–162.
[33] M. Guilmard, C. Pouillerie, L. Croguennec, C. Delmas, Solid State Ionics 160 (2003) 39–50.
[34] S.H. Park, K.S. park, Y.K. Sun, K.S. Nahm, Y.S. Lee, M. Yoshio, Electrochim. Acta 46 (2001) 1215–1222.